Chapter (6)

Results and discussion

Chapter (6)

Results and discussion

The present work represents a theoretical and experimental study of the flow of a viscoelastic fluid in the annular region between two eccentric spheres . Therefore , the results of this work is delivered into two main parts ; namely theoretical investigations of the flow field and an experimental set up of a rheometer based on this boundary value problem. Some experimental measurements were carried out using some specific fluids .

The theoretical part deals with the flow of a non-Newotonian fluid of grade two in the annular region between two eccentric spheres . Second-order fluid creates secondary flow which may be described by a stream function $\psi_2(\alpha,\beta)$. The equations of motion of second-order fluid and their solutions are outlined in the second and third chapters of the present thesis . The resultant forces and torques , up to the second-order, acting on the boundaries are described in chapter four.

Based on the previous calculations,the eccentric spheres rheometer is designed which allows the determination of the combined second-order coefficient $(\alpha_2 + 2\alpha_1)$ besides the viscosity coefficient μ .

The experimental idea of this device and a detailed description of the set up is given in the fifth chapter of the present work. The measurements of the viscosity μ of the 80/20 glycerin/water at different eccentricities by the eccentric spheres rheometer has been obtained.The first normal stress difference as well as the viscosity parameters for Non-Newtonian fluids (polyacrylamide , polystyrene,...) are also

investigated . A comparison of the obtained results with the experimental data delivered with other rheometers in recent texts are viewed [41] .

6-1. Results of the theoretical calculations

The velocity field for a fluid of grade one (Newtonian fluid) is a stationary field with a single velocity component $W_1(\alpha,\beta)$ in the $\hat{\varphi}$-direction .For a fluid of grade two , which is the main goal of the present theoretical work , the equations of motion reduces to a pair of partial differential equations ; namely

(i) The harmonic vector equation

$$\nabla^2(W_2(\alpha,\beta)\hat{\varphi}) = 0 \quad , \tag{6-1}$$

with the boundary conditions

$$\left.\begin{aligned} w_2 &= \begin{Bmatrix}0\\0\end{Bmatrix} \text{ at } \beta = \begin{Bmatrix}\beta_1\\\beta_2\end{Bmatrix} \\ w_{2,\beta} &= \begin{Bmatrix}0\\0\end{Bmatrix} \text{ at } \beta = \begin{Bmatrix}\beta_1\\\beta_2\end{Bmatrix} \end{aligned}\right\} \tag{6-2}$$

which has the solution

$$W_2(\alpha,\beta) = 0 \quad , \tag{6-3}$$

all over the domain of motion , and

*(ii)*The biharmonic vector equation

$$\nabla^4\left(\frac{\hat{\varphi}\psi_2}{h\sin\alpha}\right) = \frac{16(\alpha_1+\alpha_2)c^2}{\mu\, sh^2\frac{3}{2}\delta}\rho(\alpha,\beta)\hat{\varphi} \ , \tag{6-4}$$

with the imposed boundary conditions given by

$$\left.\begin{aligned}\psi_2 &= \begin{Bmatrix}0\\0\end{Bmatrix} \text{ at } \beta = \begin{Bmatrix}\beta_1\\\beta_2\end{Bmatrix}\\ \psi_{2,\beta} &= \begin{Bmatrix}0\\0\end{Bmatrix} \text{ at } \beta = \begin{Bmatrix}\beta_1\\\beta_2\end{Bmatrix}\end{aligned}\right\}, \tag{6-5}$$

where,

$$\rho(\alpha,\beta) = 9h^{-4}\sin\alpha\Big\{\frac{h}{c}sh\beta\Big[\sin^2\alpha(-2sh^2\tfrac{3}{2}(\beta-\beta_2)-\tfrac{3}{4})+2\cos\alpha\,(ch\beta\,sh^2\tfrac{3}{2}(\beta-\beta_2) + sh\beta\,sh3(\beta-\beta_2)\Big]+2\cos\alpha\,sh\beta\,ch^2\tfrac{3}{2}(\beta-\beta_2)-sh3(\beta-\beta_2)\Big\},$$

which specifies the second-order stream-function $\psi_2(\alpha,\beta)$ which allows the determination of the α and β-components of the second-order velocity field .

The solution of Eq.(6-4) is given by

$$\psi_2(\alpha,\beta) = \frac{9h^2\sin^2\alpha}{4\pi}\Big\{\ln(\frac{ch\beta+1}{ch\beta-1})\Big[f_1(\beta)-e^{\beta}\cos\alpha[f_2(\beta_0)]_{\beta}^{\beta_1}-e^{-\beta}\cos\alpha[f_3(\beta_0)]_{\beta_2}^{\beta}\Big]+f_8(\beta) + e^{\beta}[\cos\alpha f_4(\beta_0)+\sin\alpha f_5(\beta_0)]_{\beta}^{\beta_1}+e^{-\beta}[\cos\alpha f_6(\beta_0)+\sin\alpha f_7(\beta_0)]_{\beta_2}^{\beta} + q_1(\alpha)\frac{h^3}{c^3}+q_2(\alpha)\frac{h}{c}(ch\beta+\cos\alpha)sh^3\beta+q_3(\alpha)\frac{h}{c}sh\beta+q_4(\alpha)\Big\}. \tag{6-6}$$

where the functions $f_i(\beta)$; $i = 1,2,.....,8$ are respectively given by Eqs.(3-24a),(3-24b),....and (3-24h), and the coefficients $q_j(\alpha)$; $j = 1,2,3$ and 4 are respectively given by Eqs. (3-31a), (3-31b) , (3-31c) and (3-31d) .The present solution of the equation of motion within the second-order approximation gives the stream-function

$\psi_2(\alpha,\beta)$ which causes a secondary flow superimposed on the primary flow , which comes from the first order velocity field $W_1(\alpha,\beta)$.

Instead of (x,y,z) explicit form , the ($\rho - Z$) coordinates are used (see on the appendix) for plotting the family of streamlines which are satisfying the condition , $\psi_2(\alpha,\beta) =$ constant . In Figure (6-1) the representation of these streamlines in the region of flow $\beta_2 < \beta < \beta_1$ are plotted . The map of streamlines shows a specific symmetry about the axis of rotation;i.e.the Z-axis . The inner and outer spheres in the figure are the surfaces representing the equations $\psi_2(\alpha,\beta) = 0$.

The general streamlines of the fluid particles due to both of the primary and secondary flows can be visualized by combining the primary motion ; which takes a circular path about the Z-axis ,and the loops of the streamlines mapped onto ρZ-plane . In view of a specific particle located in a specific circular primary path , when exposed to the additional secondary motion it will draws a closed loop .Since the secondary motion is usually much slower than the primary one ,the secondary loop is exposed to be closed after several primary rotations.

Based on the outlined theoretical calculations , the stress components and hence the resultant forces and torques on the boundaries are determined . The resultant torque , force and the rate of deformation are expressed in terms of geometrical parameters , which are appropriate for practical purposes . The first measurable quantity is the resultant torques acting on the outer and inner spheres β_2 and β_1; respectively , are given by

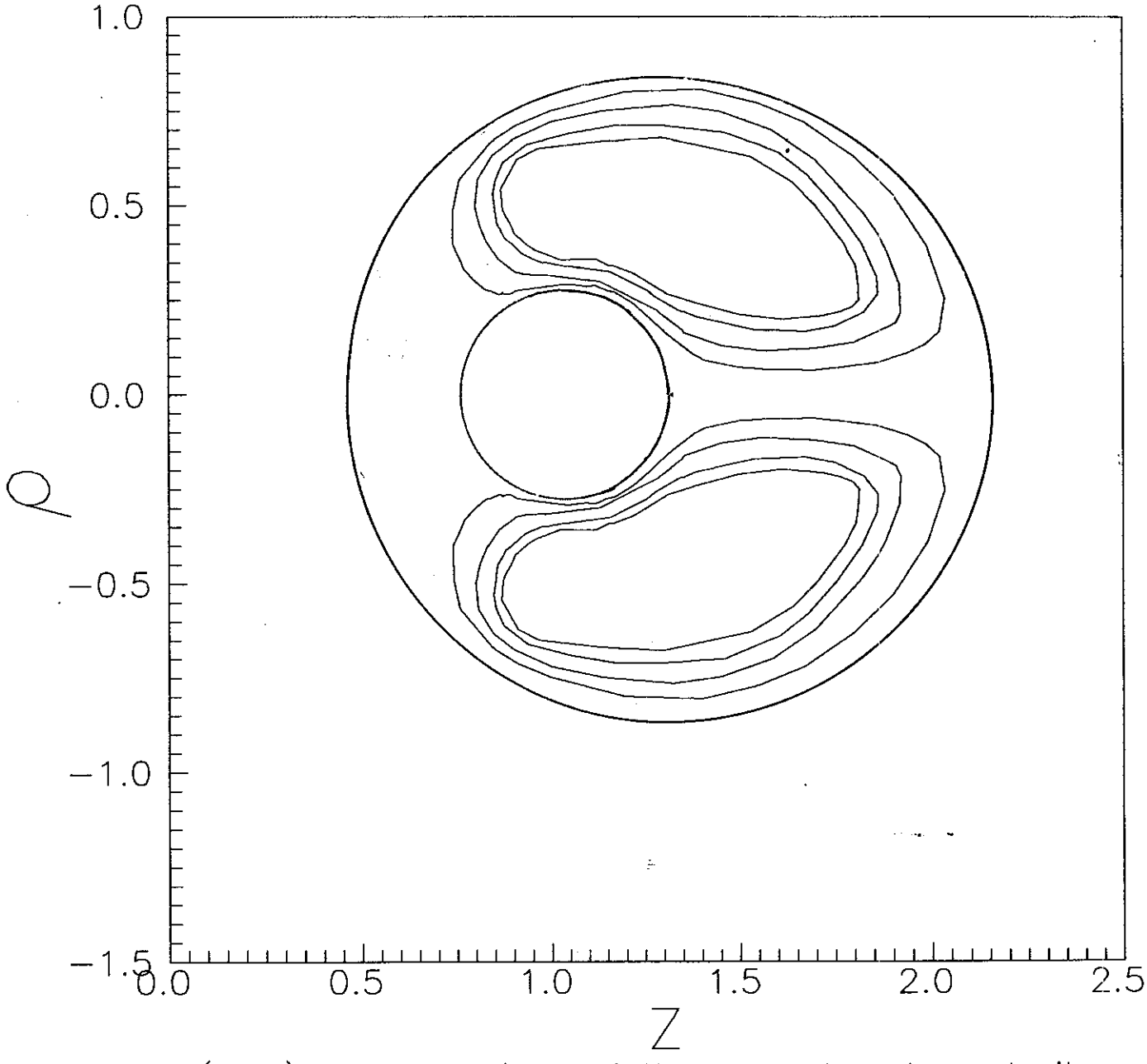

Fig.(6−1)The streamlines of the second−order velocity in $\rho-z$ coordinates .

$$M|_{\beta_2} = M \,, \tag{6-7}$$

$$M|_{\beta_1} = [M(.5+\tau_1)+\tau_2] \quad , \tag{6-8}$$

$$M = M_o \sum_{n=1}^{\infty} \frac{2^{2n} n(n+1)(2r\varepsilon)^{2(n-1)}(1-r^3)D^3}{k^{2n+1}-(Bn)^{2n+1}} \quad , \tag{6-9}$$

where,

$$M_o = -8\pi\Omega\mu \frac{R_1^3}{1-r^3} \tag{6-10}$$

= the torque in the concentric case

the functions τ_1, τ_2, D, k and B are geometrical functions which depend only on the geometrical parameters ε, R_1 and R_2 . These functions are given by Eqs.(4-52) ,(4-53), (4-40),(4-41) and (4-50) ; respectively .

The second measurable quantity is the resultant force acting on the outer sphere β_2 in the direction of the common axis of rotation such that it tries to restore the concentric position and it is given by the relation

$$F_z|_{\beta_2} = \Omega^2[(\alpha_2+2\alpha_1)F_1+\mu F_2] \tag{6-11}$$

where, F_1 **and** F_2 are geometrical functions given by Eqs.(4-39) and (4-43) respectively .

The third measurable quantity is the average rate of deformation which is determined in chapter four and its final form is given as

$$\bar{\dot{\gamma}}(\beta_2)=\frac{1.2\sqrt{2}}{\pi\nu(J+(1-r\sqrt{L(1-\varepsilon^2)})}\left[\left(\frac{J}{2\varepsilon}+1\right)^{2.5}-\left(\frac{J}{2\varepsilon}-1\right)^{2.5}\right] \qquad (6\text{-}12)$$

where, J , ν **and** L are geometrical functions given by Eqs. (4-48), (4-56) and (4-57); respectively .

The present theoretical and experimental torque data are plotted versus the eccentricity ε at different angular velocity Ω ,where the radius ratio , r=0.6 , Fig. (6-2) . The data obtained show a good fitting with the theoretical calculations particulary at the moderate eccentricities .

Munson [18] solved the present problem for Navier-Stokes fluid . He employed the usual spherical polar coordinates for the solution of the equation of motion . Since this system is not adequate for the present boundary value problem , a series of approximations is used to get the final solution . Menguturk and Munson [19] constructed an experimental set up to measure the torque on the outer sphere in order to compare it with their theoretical formula .This formula , expressed in terms of the same parameters employed in the present work., has the form

$$\frac{(M-M_o)}{M_o}=\frac{3r^3(1-r)^2}{(1-r^3)(1-r^5)}\varepsilon^2 . \qquad (6\text{-}13)$$

Noteworthy is that in the case of Navier-Stokes fluid, the toque about the axis of symmetry is the only effect which appears to act on the outer sphere . This tourque is being the first -order term in the case of

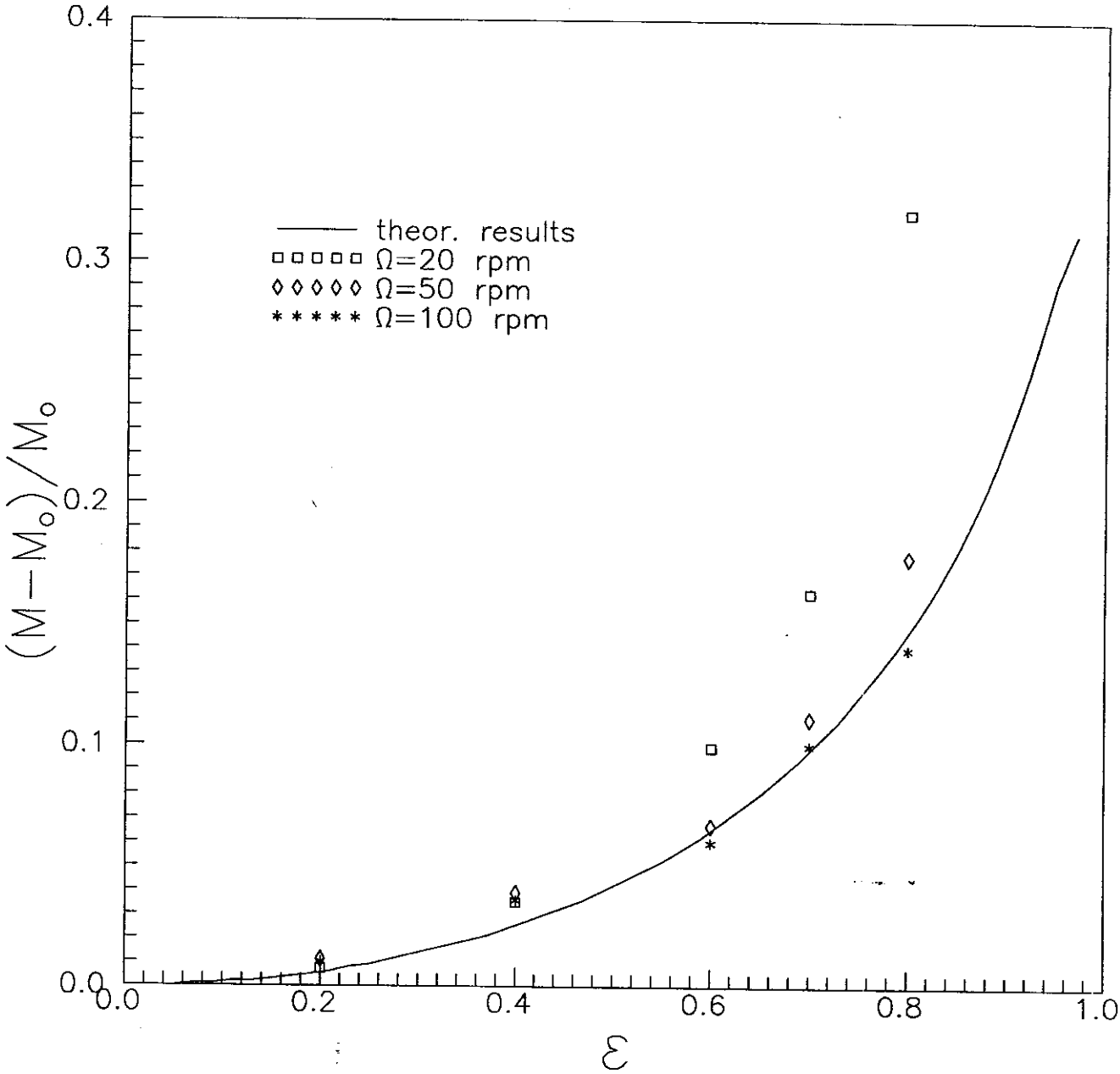

Fig.(6-2)The torque ratio $(M-M_o)/M_o$versus the eccentricity ε,at r=0.6. The solid line and symbols represent the present theoretical and experimental results at different angular velocity Ω.

viscoelastic fluid . The theoretical data obtained in the present work , Eq.(6-7), in addition to the theoretical data due to Munson ,Eq.(6-13) , are presented in Fig.(6-3) in comparison with the experimental data due to Menguturk and Munson [19] . Our theoretical curves show a better fitting to the experimental data than those due to Munson specially at large values of ε .These deviations may be attributed to the approximations made to fit the solution in terms of spherical polar coordinates of the boundary value problem . To have better insight , we give an approximate form for Eq.(6-7) for small eccentricity ,

$$\frac{(M-M_o)}{M_o} = \frac{3r^3(1-r^3)}{(1+r)^2(1-r^5)}\varepsilon^2 \quad . \qquad (6\text{-}14)$$

Equations (6-13) and (6-14) are basically different , however, both equations reduce to $M = M_o$ when $\varepsilon = 0$;i.e. both equations reduced to the concentric case .

Finally ,the investigation of the theoretical calculations in the present work show that the velocity field $\underline{\dot{x}}$, up to the second-order of approximation, for a viscoelastic fluid performing stationary flow in the annular region between two eccentric spheres when the inner sphere is rotating with angular velocity Ω and the outer sphere is kept at rest, is given by

$$\underline{\dot{x}} = \Omega W_1(\alpha,\beta)\hat{\varphi} + \Omega^2 \underline{u}_2(\alpha,\beta) + O(\Omega^3) . \qquad (6\text{-}15)$$

The scalar field $W_1(\alpha,\beta)$ is the primary flow ,Eq.(2-21) , and it is being in the $\hat{\varphi}$ direction ; i.e. in the direction of the axis of rotation . The

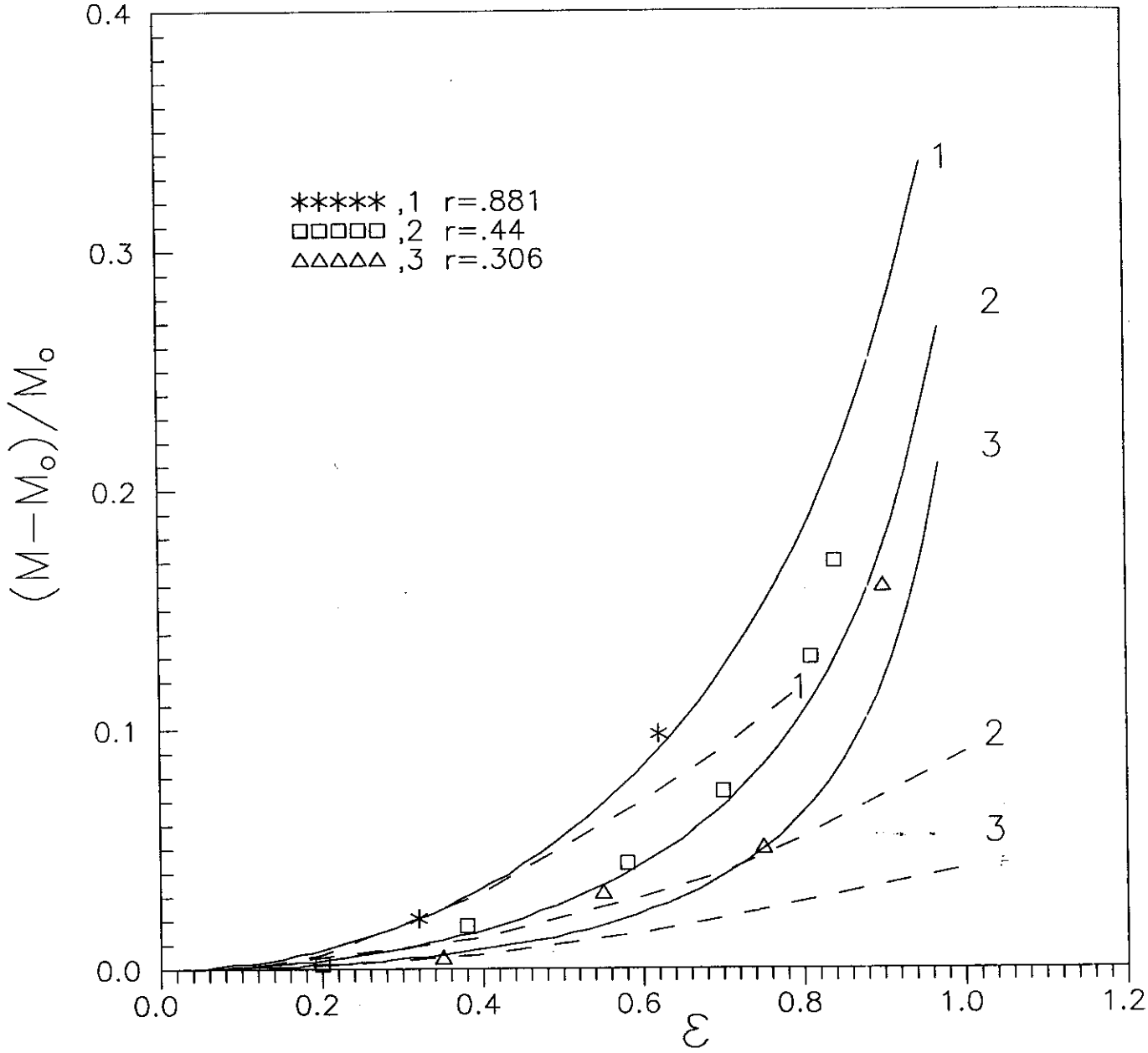

Fig.(6–3)The torque ratio $(M-M_o)/M_o$ plotted versus the eccentricity ε in comparison with Munson [19] .where r is radius ratio R_1/R_2.Dashed line and symbols represent theoretical and experimental data from Munson.

vector field $\underline{u}_2(\alpha,\beta)$ is being a secondary flow field which superimposed on the primary flow $W_1(\alpha,\beta)$ and the components of $\underline{u}_2(\alpha,\beta)$ are specified by a second-order stream-function $\psi_2(\alpha,\beta)$,Eq.(3-25) .

Based on the results of $\dot{\underline{x}}$, Eq.(6-15), the distribution of stresses and hence the resultant forces and torques at the boundaries are investigated . Therefore , we conclude that :

(i)The resultant torque about an axis of symmetry can be used to determine the viscosity of the fluid . When the eccentricity ε tends to zero the eccentric torque reduced to the known formula of the concentric case [40] ,

$$\lim_{\varepsilon=0} M = M_o \sum_{n=1}^{\infty} \frac{2^{2n} n(n+1)(2r\varepsilon)^{2(n-1)}(1-r^3)D^3}{k^{2n+1}-(Bn)^{2n+1}} = M_o$$

where,

$$M_o = -8\pi\Omega\mu \frac{R_1^3}{1-r^3}$$

= the torque in the concentric case

(ii)The resultant force acting on the outer sphere can be used to determine a combination of the second-order material parameter $[\alpha_2 + 2\alpha_1]$. This force disappears for the case of two concentric spheres;i.e.

$$\lim_{\varepsilon=0} F_z = \Omega^2[(\alpha_2 + 2\alpha_1)F_1 + \mu F_2] = 0 .$$

6-2.Experimental Tests

For the examination of the reliability of the results obtained with the new device , measurements were carried out with a suitable Newtonian fluid; namely an 80/20 glycerin-water mixture. Figure(6-4) shows that the viscosity values , calculated using the measured torque $M(\alpha,\beta_1)$, are independent of the angular velocity Ω . These shear viscosity values are , however , not restricted to measurements with small relative eccentricities but can be realized up to values $\varepsilon = 0.8$. In other words the independence of the shear viscosity upon the angular velocity Ω is being for all eccentricities ; Fig.(6-4).

Noteworthy,for these Newtonian (viscous) fluids,in the respective experiments the force F_z obtained with the eccentric spheres rheometer are always disappearing; therefore no graphs of the first normal stress difference coefficient values are added .

For Non-Newtonian fluids ; namely 0.3 % polyacrylamide in water the relation between the shear viscosity values μ and the angular velocity Ω ,Fig.(6-5) , at two different values of ε ,show that μ is gradually decreasing with increasing Ω . The same behavior is obtained in the case of the first normal stress difference $[\alpha_2 + 2\alpha_1]$ versus the average shear rates $\dot{\bar{\gamma}}$; as shown in Fig.(6-6).

Subsequently, a solution having 0.3 % polyacrylamide in 50/50 glycerin -water mixture has been tested . Figures (6-7) and (6-8) show that, both the viscosity and the first normal stress difference coefficient

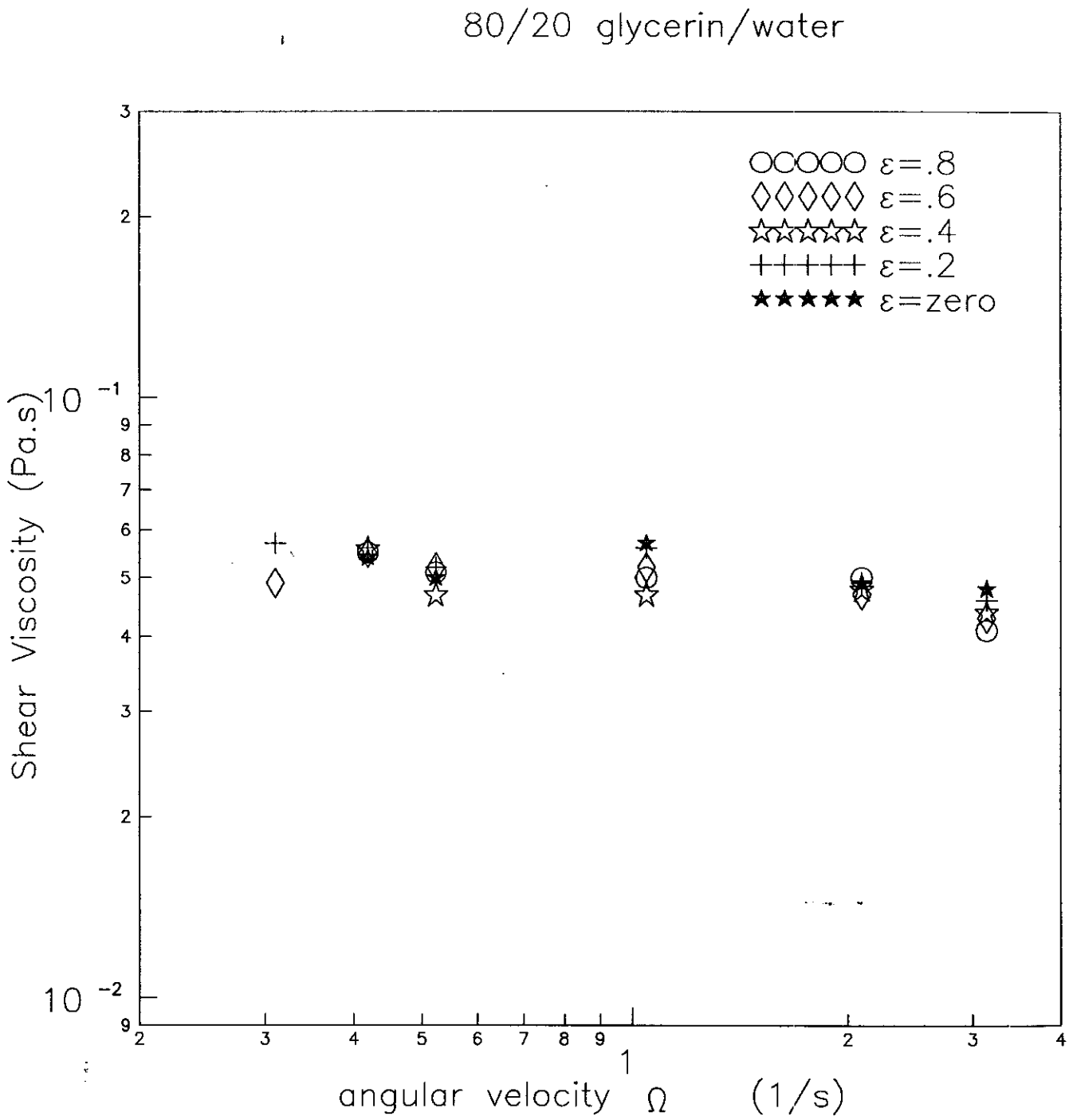

Fig.(6−4)The shear viscosity versus the angular velocity .

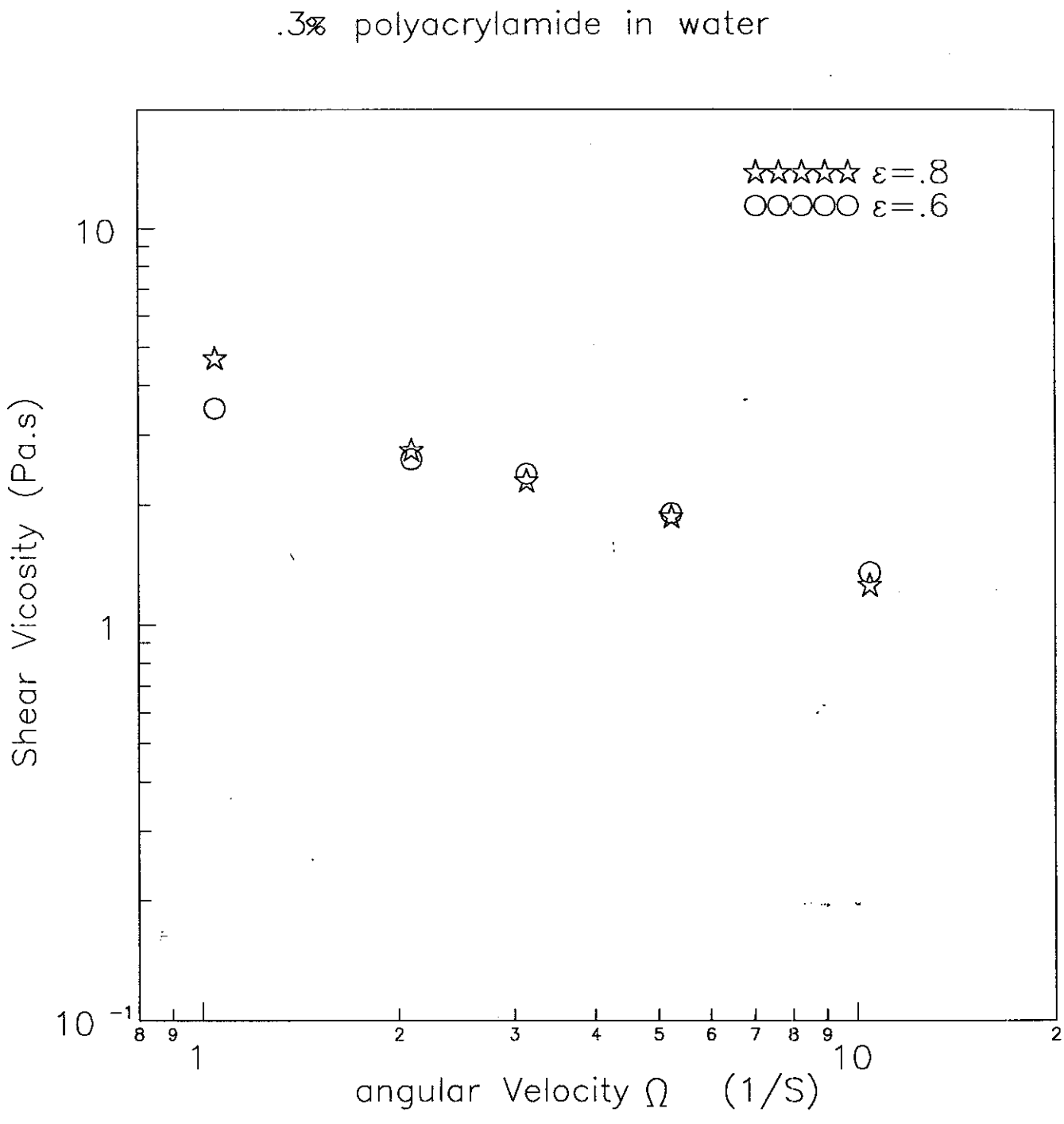

Fig.(6−5)The shear viscosity versus the angular velocity .

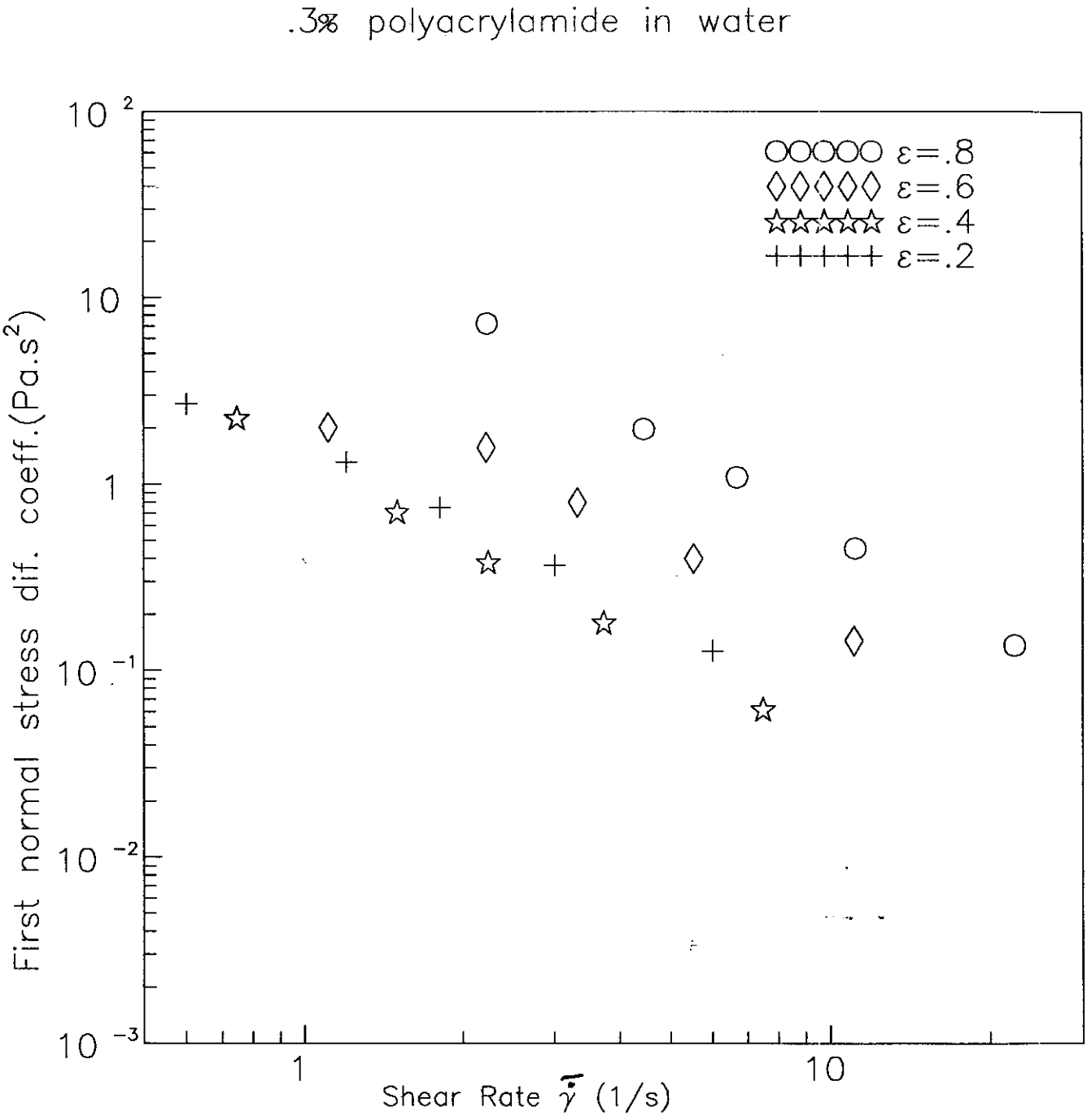

Fig.(6–6)The first normal stress difference coefficient versus the shear rate.

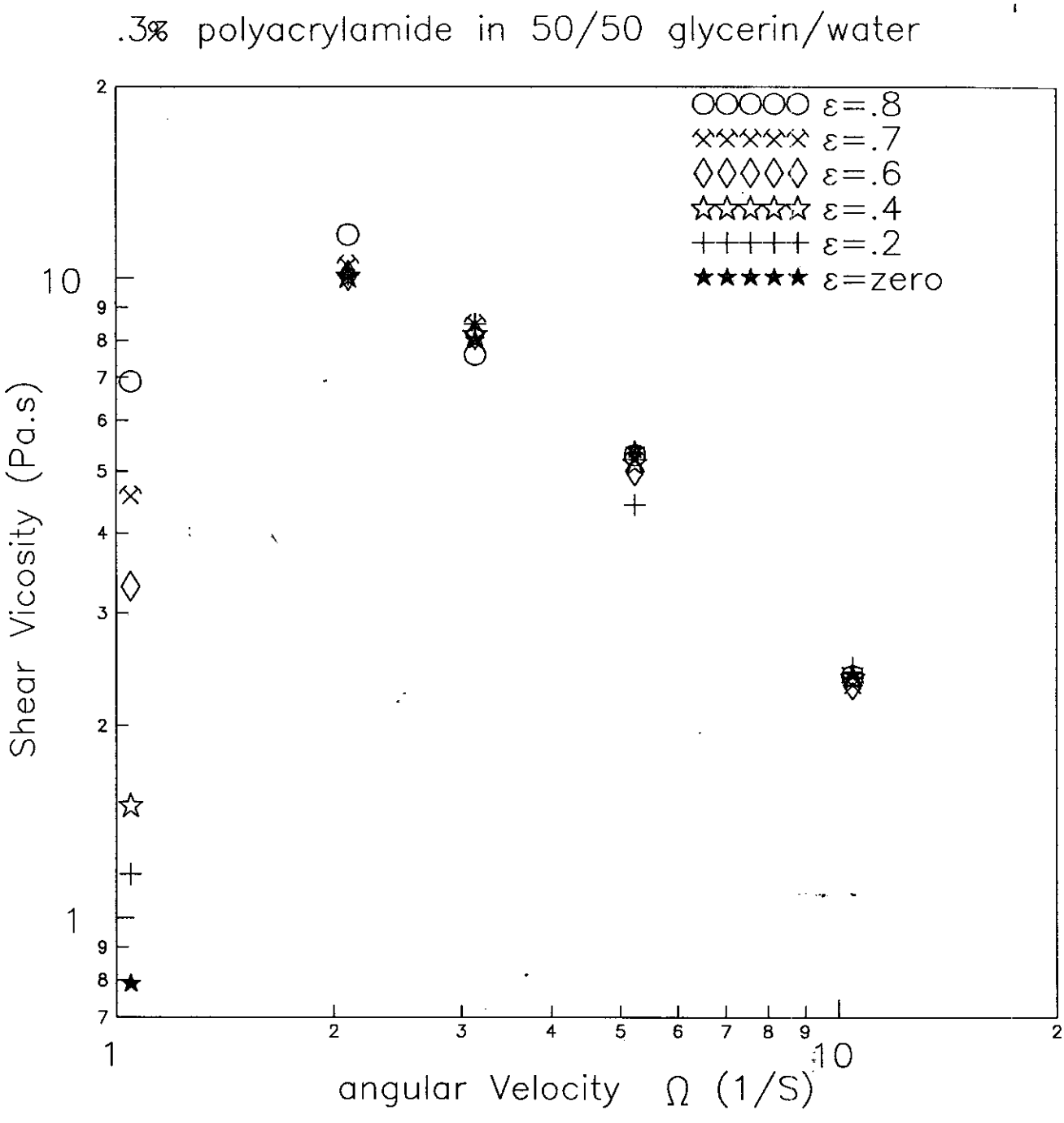

Fig.(6−7)The shear viscosity versus the angular velocity.

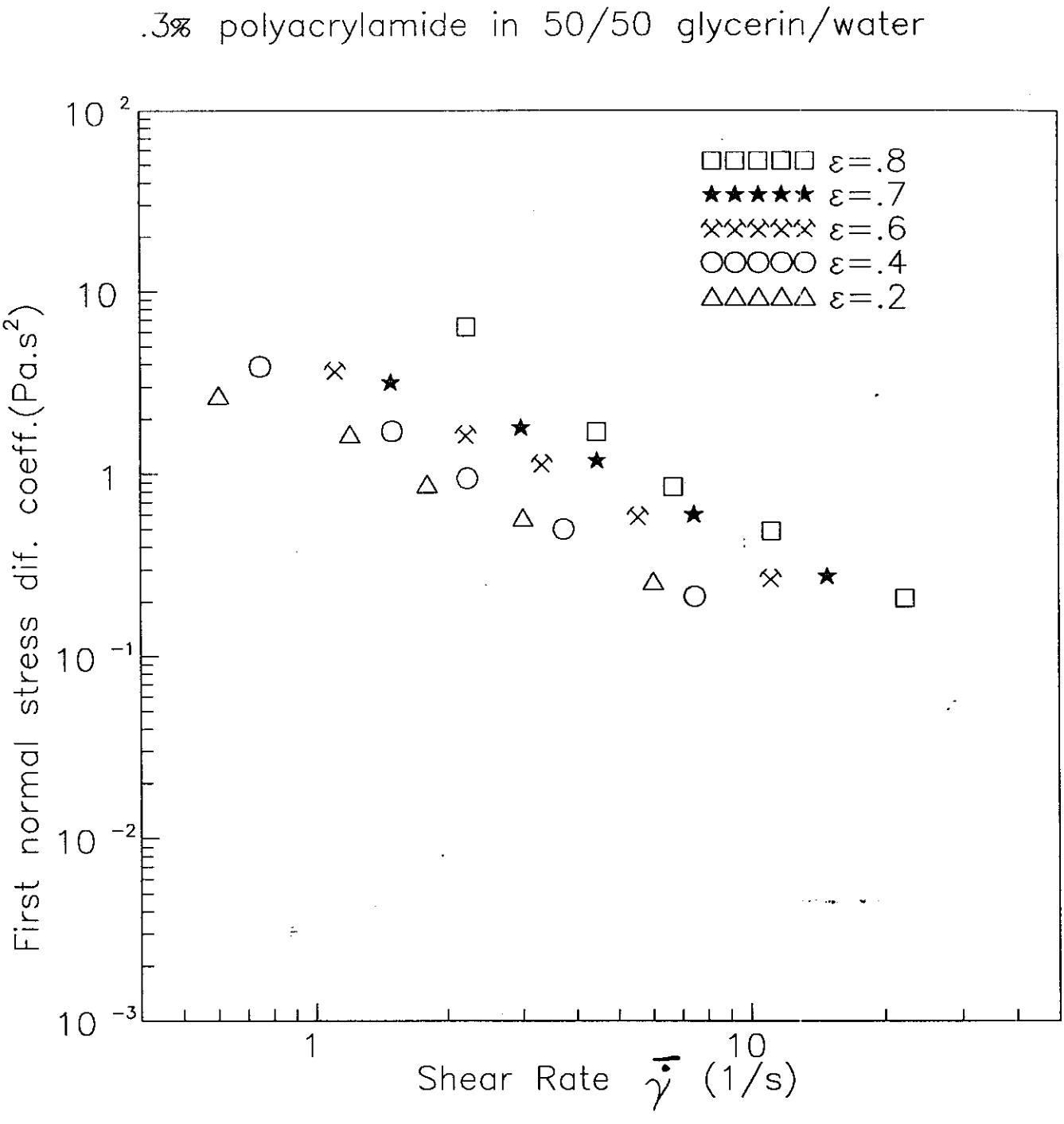

Fig.(6-8)The first normal stress difference coefficient versus the shear rate.

values have the same behavior as polyacrylamide in glycerin/water. This behavior is being that ,for constant ε, μ is decreasing with increasing Ω . The same manner for $[\alpha_2 + 2\alpha_1]$ with $\dot{\gamma}$ is shown. Besides that, for shear viscosity values the obtained measurements have a negligible difference from each other for different eccentricities up to 0.8 . But for the first normal stress difference coefficient the curves have diverged up to $\varepsilon = 0.7$ specially for small values of $\dot{\gamma}$.

The torque and force data are plotted versus the angular velocity Ω for the same solution given in Figs.(6-9) and (6-10); respectively .It is noticed that , the torque $M(\alpha,\beta_1)$ abruptly increases for the case of small angular velocities which promotes asymptotic value at the higher angular velocities . On the other hand the force $F_Z(\alpha,\beta_2)$ increases monotonically with increasing either the eccentricity ε or the angular velocity Ω.

For the case 1.5 % of polyacrylamide in a 50/50 glycerin -water mixture, the shear viscosity strongly decreases with increasing angular velocity Ω while it shows eccentricity independent, Fig.(6-11), . It is noticed that, the general behaviour of the first normal stress difference coefficient $[\alpha_2 + 2\alpha_1]$ decreases with increasing the shear rate,Fig.(6-12), and is nearly independent of the eccentricity . In addition the present data coincide with those obtained by other investigators [41] at the higher shear rate ; the observed deviation in $[\alpha_2 + 2\alpha_1]$ at the small shear rate can be attributed to the expected vibrations at the small rotation speeds.